EFFECT OF RADIATION ON MAGNETO HYDRODYNAMICS FLOW OF JEFFREY FLUID OVER AN INFINITE VERTICAL PLATE

R. Lakshmi Devi[1], Konduru Venkateswara raju[2], E. Sudhakara[3], Mopuri Obulesu[4], P. Jayalakshmi[5], M. Umamaheswar[6*]

ArticleHistory:Received:08.04.2023 **Revised:**16.06.2023 **Accepted:**20.07.2023

Abstract:

We've got mentioned unsteady MHD rotating glide of an electrically engaging in, viscous, incompressible and optically thick radiating Jeffrey's fluid beyond a rapidly vertical shifting porous plate while temperature of the plate has a quickly ramped profile. Analytical answers of the governing equations are received by way of Laplace remodel method. The ideal solution is likewise received in case of unit Schmidt range. The analytical terms for pores and skin friction and Nusselt number are derived for each ramped temperature and isothermal plates. Sherwood variety is likewise obtained. The speed, temperature and awareness are displayed graphically whereas pores and skin friction, Nusselt variety and Sherwood number are supplied in tabular shape.

Keywords: MHD Flows, Porous Medium, Convection Flows, Vertical Plate, Ramped Temperature, Isothermal Plate.

[1]Department of Mathematics, Siddharth Institute of Engineering &Technology (Autonomous), Puttur-517 583, A.P., India.
Email: [1]lakshmi.rathiraju@gmail.com
[2]Department of Mathematic, Sri Venkateswarara College of Engineering (Autonomous), Karakambodi Road, Tirupati-517507, India,
Email:[2]venky.sakku@gmail.com
[3]Departments of Mathematics, Government Degree College, Vempalli - 516 329, A.P., India.
Email: [3]drsudhakar12@gmail.com
[4]Department of Mathematics, Siddharth Institute of Engineering &Technology (Autonomous), Puttur-517 583, A.P., India.
Email: [4]mopuriobulesu1982@gmail.com
[5]Department of Mathematics, Siddharth Institute of Engineering &Technology (Autonomous), Puttur-517 583, A.P., India.
Email: [5]jayachetu85@gmail.com
[6*]Department of Mathematics, Annamacharya Institute of Technology & Sciences, Rajampet, A.P., India-516126.
Email: [6*]umasvu8@gmail.com

***Corresponding Author**
M. Umamaheswar[6*]
[6*]Department of Mathematics, Annamacharya Institute of Technology & Sciences, Rajampet, A.P., India-516126.
Email: [6*]umasvu8@gmail.com

DOI: 10.31838/ecb/2023.12.6.213

Nomenclature

u, w	fluid velocity in x and z-direction
g	Acceleration due to gravity
k^*	Rossland mean absorption coefficient
C_p	specific heat at constant pressure
k	Thermal conductivity of the fluid
K_1	Permeability of the porous medium
q_r	radiative flux vector
D	chemical molecular diffusivity
q	the velocity vector,
U_0	uniform velocity of the plate
M	Hartmann number,
R	Rotation parameter,
K	Permeability parameter,
Gr	thermal Grashof number,
Gc	mass Grashof number,
Pr	Prandtl number
N	thermal radiation parameter and
Sc	the Schmidt number
$H(t\text{-}1)$	unit step function
$erfc(x)$	complementary error function

Greek symbols:

β	volumetric coefficient of thermal expansion
β^*	volumetric coefficient of expansion for species concentration
μ_e	the magnetic permeability
Ω	Uniform angular velocity
σ^*	Stefan–Boltzmann constant.
ν	Coefficient of kinematic viscosity
ρ	fluid density
σ	electrical conductivity
θ	fluid temperature
ϕ	species concentration

1. Introduction

Natural convection flow, propelled by thermal and solutal buoyant forces through items with unique geometries in a fluid-saturated porous medium, is used in a wide variety of natural occurrences and commercial applications. Industrial emissions can contaminate atmospheric flows, making it impossible to attain truly pure air or water. Thermal and solute buoyancy forces are becoming more sophisticated due to temperature or concentration or an amalgamation of those two factors [1]. This configuration is used in a wide variety of applications, including but not limited to heat exchange mechanism devices, to regulate the temperature of molten alloys with other elements, sealing structures, significant oil reservoirs, the filtration process, chemically produced catalytic reactors and procedures, nuclear waste recovery and so on. As a consequence of the significance of fluid float issues, an extensive number of researchers [2-10] have committed a great agreement of time and energy to studying them. Various investigators have been dedicating an immense amount of time and energy to the investigation of natural convection boundary layer flow across a variety of geometrical entities with heat and mass transfer in porous and non-porous materials [11-15].

Muhammad [17] examined the behavioural patterns of the flow near the hydrodynamic stagnation point with a non uniform internal heat source/sink. Heat transfer was discussed by Azeem et al. [18] in the context of an axisymmetric flow that is unstable on a radially stretchable sheet.Turkyilmazoglu[19] described the micropolar fluid's MHD float over a porous substrate.Baag et al.[20] have demonstrated a brief concept of MHD flow by employing the second law of thermodynamics and utilising dissipation in the forms of Darcy, viscous, and Joule energy. MHD axisymmetric flow of energy-regulating fluid over a stretching sheet was analysed under convective surface conditions in a study by Ahmed et al.[21]. Using the slip effect, Fauzi et al.[22] discussed the effect of heat transmission on the stagnation factor consideration as it moves past a nonlinearly contracting sheet. Hakeem et al.[23] studied the motion of a Nano fluid via a porous floor using 2nd order MHD slip. Using viscous dissipation, Ruchika et al.[24] described how a few MHD nanofluid solutions can float through a porous surface. The fantastic idea of the flow was put to the test by Bhattacharya [25-27] on a shrinking surface. When a sheet is stretched or compressed, the stagnation factor can cause the sheet to change shape, which Gangadhar et al. [28] studied. In their study, Maria and her colleagues [29] delved into the fascinating world of MHD glide in Jeffrey Fluid. They explored the effects of a curved stretching floor and homogeneous-heterogeneous reactions, adding a new layer of complexity to this intriguing phenomenon.In a daring scientific pursuit, Sandeep and Sulochana delved into the intricacies of non-Newtonian nanofluids' heat transfer dynamics. Their study focused on the behaviour of these fluids over a stretching exterior, where heat supply or sink was non-uniform. The flow of a Jeffrey fluid past an exponentially stretching sheet was investigated by Ahmad et al. [31] under mixed convective MHD conditions. Hayat et al. [32] delved into the intriguing topic of MHD stagnation point float of Jeffrey fluid, taking into account the effects of viscous dissipation and Joule heating. In their study, Das et al. [33] delved into the captivating phenomenon of Jeffrey fluid drift over a stretching sheet, taking into account the intriguing factors of melting heat switch and floor slip. In this study, the abruptly vertically moving porous plate and its rapidly ramping temperature profile are considered in the context of the unsteady MHD rotating flow of an electrically conductive, viscous, incompressible, and optically thick radiating Jeffrey's fluid. Raju et.al.[35-37] examined the different effects of radiation effects in MHD.

Formulation and Solution of the Problem

We explored the exciting possibilities of studying the unsteady hydromagnetic flow of a fluid that is electrically functioning, viscous, incompressible, and optically thick, over an infinite vertical plate that has been embedded in a uniform porous medium in a rotating system. Behold, the very embodiment of the problem's physical configuration, as depicted in the illustrious Fig. 1.

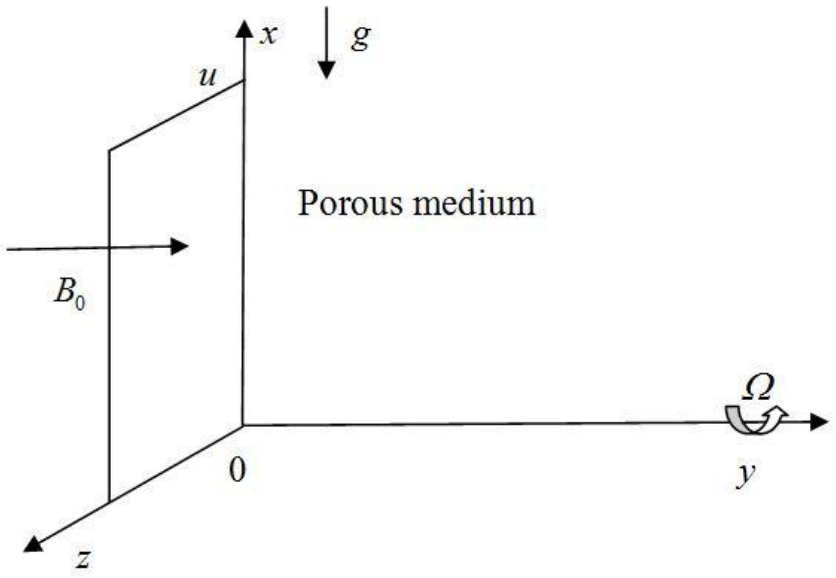

Fig 1. The physical presentation of the problem

Co-ordinate mechanism is chosen, the x-axis is taken to run parallel and upward from the plate, whereas the y-axis is taken to run perpendicular to the plane of the plate in the fluid. Along a path that is parallel to the y-axis, a transversely directed magnetic field B_0 that is constant in intensity is generated.As if in a synchronised movement the fluid and surface rotate together with an uniform angular velocity around the y-axis.At the outset, the fluid and plate are in a state of steady and are being upheld at an even temperature. Concentration is held constant at both the plate's surface and on each component of the fluid underneath. At time t , plate starts moving in x-path with uniform pace in its own plane. The temperature of plate is raised or decreased while t, and it is maintained at uniform temperature when (being characteristic time). Also, at time t , species concentration at the surface of the plate is raised to uniform species awareness and is maintained thereafter. Since plate is of infinite volume in x and z guidelines, all bodily portions besides pressure depend on y and t only.

The governingequationsforflow through porousmediuminarotatingframearegivenby

$$\frac{\partial u}{\partial t}+2\Omega w=\frac{\nu}{1+\lambda_1}\left(1+\lambda_2\frac{\partial}{\partial t}\right)\frac{\partial^2 u}{\partial y^2}-\frac{\sigma B_0^2}{\rho}u-\frac{\nu}{K_1}u+g\beta(\theta-\theta_\infty)+g\beta^*(\phi-\phi_\infty) \quad (1)$$

$$\frac{\partial w}{\partial t}-2\Omega u=\frac{\nu}{1+\lambda_1}\left(1+\lambda_2\frac{\partial}{\partial t}\right)\frac{\partial^2 w}{\partial y^2}-\frac{\sigma B_0^2}{\rho}w-\frac{\nu}{K_1}w \quad (2)$$

$$\rho C_p\frac{\partial\theta}{\partial t}=k\frac{\partial^2\theta}{\partial y^2}-\frac{\partial q_r}{\partial y} \quad (3)$$

$$\frac{\partial\phi}{\partial t}=D\frac{\partial^2\phi}{\partial y^2} \quad (4)$$

Initialandboundaryconditionsare

$u = w = 0, \theta = \theta_\infty, \phi = \phi_\infty$ for $y \geq 0$ and $t \leq 0$, (5)

$u = U_0, w = 0$ at $y = 0$ for $t > 0$, (6)

$\theta = \theta_\infty + (\theta_w - \theta_\infty)\frac{t}{t_0}$ at $y = 0$ for $0 < t \leq t_0$, (7)

$\theta = \theta_w$ at $y = 0$ for $t > t_0$, (8)

$\phi = \phi_w$ at $y = 0$ for $t > 0$, (9)

$w \to 0; \theta \to \theta_\infty; \ \phi \to \phi_\infty$ as $y \to \infty$ for $t > 0$. (10)

Foranopticallythickfluid,emissionandself-absorptionweadoptedtheRosselandapproximationforradiativefluxvector q_r .

$$q_r = -\frac{4\sigma^*}{3k^*}\frac{\partial \theta^4}{\partial y}, \quad (11)$$

Assumesmalltemperaturedifferencebetweenfluidtemperatureθandfreestreamtemperature θ_∞ , θ^4 isexpandedinTaylorseriesaboutfreestreamtemperature θ_∞ tolinearizeequation(11),afterneglectingsecondandhigherordertermsin $\theta - \theta_\infty$,

$$\theta^4 \cong 4\theta_\infty^3\theta - 3\theta_\infty^4 \quad (12)$$

Eq.(3)withhelpofEqs.(11)and(12)reducesto

$$\frac{\partial \theta}{\partial t} = \frac{k}{\rho C_p}\frac{\partial^2 \theta}{\partial y^2} + \frac{1}{\rho C_p}\frac{16\sigma^*\theta_\infty^3}{3k^*}\frac{\partial^2 \theta}{\partial y^2} \quad (13)$$

We introduce the non-dimensional variables,

$$y^* = \frac{y}{U_0 t_0}, u^* = \frac{u}{U_0}, w^* = \frac{w}{U_0 t_0}, t^* = \frac{t}{t_0}, \ \theta^* = \frac{\theta - \theta_\infty}{\theta_w - \theta_\infty}, \phi^* = \frac{(\phi - \phi_\infty)}{(\phi_w - \phi_\infty)}$$

Making use of non-dimensional variables, Eqs. (1), (2), (4) and (13) are

$$\frac{\partial u}{\partial t} + 2R^2 w = \frac{1}{1+\lambda_1}\left(1 + \lambda\frac{\partial}{\partial t}\right)\frac{\partial^2 u}{\partial y^2} - \left(M^2 + \frac{1}{K}\right)u + \mathrm{Gr}\theta + \mathrm{Gc}\phi \quad (14)$$

$$\frac{\partial w}{\partial t} - 2R^2 u = \frac{1}{1+\lambda_1}\left(1 + \lambda\frac{\partial}{\partial t}\right)\frac{\partial^2 w}{\partial y^2} - \left(M^2 + \frac{1}{K}\right)v \quad (15)$$

$$\frac{\partial \theta}{\partial t} = \frac{(1+N)}{\mathrm{Pr}}\frac{\partial^2 \theta}{\partial y^2} \quad (16)$$

$$\frac{\partial \phi}{\partial t} = \frac{1}{\mathrm{Sc}}\frac{\partial^2 \phi}{\partial y^2} \quad (17)$$

Where

$M^2 = \frac{\sigma B_0^2 \nu}{\rho U_0^2}$ is the Hartmann number, $R^2 = \frac{\nu\Omega}{U_0^2}$ is the rotationparameter, $K = \frac{K_1 U_0^2}{\nu^2}$ is permeabilityparameter, $\lambda = \frac{\lambda_2 U_0^2}{\rho\nu^2}$ is the Jeffrey's fluid parameter, $\mathrm{Gr} = \frac{g\beta\nu(\theta_w - \theta_\infty)}{U_0^3}$ is the thermalGrashofnumber, $\mathrm{Gc} = \frac{g\beta^*\nu(\phi_w - \phi_\infty)}{U_0^3}$ is the mass Grashofnumber, $\mathrm{Pr} = \frac{\nu\rho C_p}{k}$ Prandtlnumber $N = \frac{16\sigma^*\theta_\infty^3}{3kk^*}$ thermalradiationparameter and $\mathrm{Sc} = \frac{\nu}{D}$ is the Schmidtnumber.

Characteristictime t_0 isaccordingtothenon-dimensionalprocessmentionedaboveas $t_0 = \frac{\nu}{U_0^2}$.

Combining Eqs.(14)and(15) let $q = u + iw$,

$$\frac{\partial q}{\partial t} = \frac{1}{1+\lambda_1}\left(1+\lambda\frac{\partial}{\partial t}\right)\frac{\partial^2 q}{\partial y^2} - \left(M^2 + \frac{1}{K}\right)q + \mathrm{Gr}\,\theta + \mathrm{Gc}\,\phi \qquad (18)$$

|

The non-dimensional initial and boundary conditionsare

$$q = 0,\ \theta = 0,\ \phi = 0 \text{ for } y \geq 0 \text{ and } t \leq 0 \qquad (19)$$

$$q = 1 \quad \text{at } y = 0 \text{ for } t > 0, \qquad (20)$$

$$\theta = t \quad \text{at } y = 0 \text{ for } 0 < t \leq 1, \qquad (21)$$

$$\theta = 1 \quad \text{at } y = 0 \text{ for } t > 1, \qquad (22)$$

$$\phi = 1 \quad \text{at } y = 0 \text{ for } t > 0, \qquad (23)$$

$$q \to 0;\ \theta \to 0;\ \phi \to 0 \text{ as } y \to \infty \text{ for t} > 0. \qquad (24)$$

Eqs.(16),(17)and(18),aftertakingLaplacetransformandusinginitialconditions(19),reduceto

$$\frac{d^2\bar{\theta}}{dy^2} - sa\bar{\theta} = 0, \qquad (25)$$

$$\frac{d^2\bar{\phi}}{dy^2} - s\mathrm{Sc}\bar{\phi} = 0, \qquad (26)$$

$$\frac{d^2\bar{q}}{dy^2} - \lambda_3\,\bar{q} = -\frac{(1+\lambda_1)\mathrm{Gr}}{(1+s\lambda)}\,\bar{\theta} - \frac{(1+\lambda_1)\mathrm{Gc}}{(1+s\lambda)}\,\bar{\phi} \qquad (27)$$

Boundaryconditions(20)-(24) in terms of transformed variables,

$$\bar{q} = \frac{1}{s}, \bar{\theta} = \frac{(1-e^{-s})}{s^2}, \bar{\phi} = \frac{1}{s} \qquad \text{at} \quad y = 0, \tag{28}$$

$$\bar{q} \to 0, \bar{\theta} \to 0, \bar{\phi} \to 0 \qquad \text{as} \qquad y \to \infty. \tag{29}$$

SolutionsofEqs.(25)-(27)subjecttotheboundaryconditions(28)and(29)aregivenby

$$\bar{\theta}(y,s) = \frac{(1-e^{-s})}{s^2} e^{-y\sqrt{sa}}, \tag{30}$$

$$\bar{\phi}(y,s) = \frac{1}{s^2} e^{-y\sqrt{s\mathrm{Sc}}}, \tag{31}$$

$$\bar{q}(y,s) = \frac{1}{s} e^{-y\sqrt{\lambda_3}} + \frac{G_1(1-e^{-s})}{s^2(s-\beta_1)}\left\{e^{-y\sqrt{\lambda_3}} - e^{-y\sqrt{sa}}\right\} + \frac{G_2}{s(s+\beta_2)}\left\{e^{-y\sqrt{\lambda_3}} - e^{-y\sqrt{s\mathrm{Sc}}}\right\}, \tag{32}$$

Where, $\lambda_3 = \dfrac{(1+\lambda_1)\left(M^2 + (1/K) - 2iR^2 + s\right)}{1+\lambda s}, \mathrm{G}_1 = \dfrac{\mathrm{Gr}}{a-1}, \mathrm{G}_2 = \dfrac{\mathrm{Gc}}{\mathrm{Sc}-1}$,

$$\beta_1 = \frac{(1+\lambda_1)}{a-1}, \ \beta_2 = \frac{(1+\lambda_1)}{1-\mathrm{Sc}}$$

TakinginverseLaplacetransform to the Eqs. (30)–(32), we found the exactsolutionforthetemperature,concentrationandvelocity are

$$\theta(y,t) = \theta^*(y,t) - H(t-1)\,\theta^*(y,t-1) \tag{33}$$

$$\phi(y,t) = erf\left(\frac{y}{2}\sqrt{\frac{\mathrm{Sc}}{t}}\right), \tag{34}$$

$$q(y,t) = \frac{1}{2}\left[e^{y\sqrt{M_1}} erfc\left(\frac{y}{2\sqrt{t}} + \sqrt{M_1 t}\right) + e^{-y\sqrt{\lambda}} erfc\left(\frac{y}{2\sqrt{t}} - \sqrt{M_1 t}\right)\right] +$$

$$G_1[F^*(y,t) - H(t-1)F^*(y,t-1)] + G_2\ \phi^*(y,t), \tag{35}$$

The fluid problemwith $\mathrm{Sc} = 1$ correspondstowhichbothviscousandconcentrationboundarylayerthicknessesareofsimilarorderin itsmagnitude.Substituting $\mathrm{Sc} = 1$inEq. (34), thenconcentrationandvelocity are

$$\phi(y,t) = erfc\left(\frac{y}{2\sqrt{t}}\right) \tag{36}$$

$$q(y,t) = \frac{1}{2}\left[e^{y\sqrt{M_1}} erfc\left(\frac{y}{2\sqrt{t}} + \sqrt{M_1 t}\right) + e^{-y\sqrt{M_1}} erfc\left(\frac{y}{2\sqrt{t}} - \sqrt{M_1 t}\right)\right] +$$

$$G_1[F^*(y,t) - H(t-1)F^*(y,t-1)] + G_3\phi_1^*(y,t) \tag{37}$$

The solutionforthetemperatureandvelocityfortheflowpastanimpulsivelymoving thermal verticalplateisattained.

$$\theta(y,t) = erfc\left(\frac{y}{2}\sqrt{\frac{a}{t}}\right), \tag{38}$$

$$q(y,t) = \frac{(1-\gamma)}{2}\left[e^{y\sqrt{M_1}}erfc\left(\frac{y}{2\sqrt{t}}+\sqrt{M_1 t}\right)+e^{-y\sqrt{M_1}}erfc\left(\frac{y}{2\sqrt{t}}-\sqrt{M_1 t}\right)\right]$$

$$+\frac{G_1}{\beta_1}\frac{e^{\beta_1 t}}{2}\left(\left\{e^{y\sqrt{(\lambda+\beta_1)}}erfc\left(\frac{y}{2\sqrt{t}}+\sqrt{(\lambda+\beta_1)t}\right)+e^{-y\sqrt{(\lambda+\beta_1)}}erfc\left(\frac{y}{2\sqrt{t}}-\sqrt{(\lambda+\beta_1)t}\right)\right\}\right.$$

$$\left.-\left\{e^{y\sqrt{a\beta_1}}erfc\left(\frac{y}{2}\sqrt{\frac{a}{t}}+\sqrt{\beta_1 t}\right)+e^{-y\sqrt{a\beta_1}}erfc\left(\frac{y}{2}\sqrt{\frac{a}{t}}-\sqrt{\beta_1 t}\right)\right\}\right)$$

$$-G_1\lambda\,\frac{e^{\left(\frac{-1}{\lambda}\right)t}}{2}\left(\left\{e^{y\sqrt{M_1-\frac{1}{\lambda}}}\,erfc\left(\frac{y}{2\sqrt{t}}+\sqrt{(M_1-\frac{1}{\lambda})t}\right)+e^{-y\sqrt{M_1-\frac{1}{\lambda}}}erfc\left(\frac{y}{2\sqrt{t}}-\sqrt{(M_1+\beta_1)t}\right)\right\}\right.$$

$$\left.-\left\{e^{y\sqrt{\frac{-a}{\lambda}}}erfc\left(\frac{y}{2}\sqrt{\frac{a}{t}}+\sqrt{(-1/\lambda)t}\right)+e^{-y\sqrt{\frac{-a}{\lambda}}}erfc\left(\frac{y}{2}\sqrt{\frac{a}{t}}-\sqrt{(-1/\lambda)t}\right)\right\}\right)$$

$$+\gamma\;erfc\left(\frac{y}{2}\sqrt{\frac{a}{t}}\right)+G_2\,\phi^* \tag{39}$$

The skin friction components τ_x and τ_z andNusselt number are evaluated for both rampedtemperatureplate and isothermal plate; theSherwoodnumberin termsofrateofmasstransferattheplate are given by
Fortherampedtemperatureplate:

$$\tau_x + i\tau_z = \sqrt{M_1}\left(erfc\left(\sqrt{M_1 t}\right)-1\right)-\frac{1}{\sqrt{\pi t}}e^{-M_1 t}+G_1\left[F_1(0,\mathrm{t})-H(\mathrm{t}-1)F_1(0,t-1)\right]+G_2F_2(0,t) \quad (40)$$

$$Nu = 2\sqrt{\frac{a}{\pi}}\left[\sqrt{t}-\sqrt{(t-1)}H(t-1)\right] \quad (41)$$

For the isothermal plate

$$\tau_x + i\tau_z = (1-\gamma)\sqrt{M_1}\left(erfc\left(\sqrt{M_1 t}\right)-1\right)-\frac{1}{\sqrt{\pi t}}e^{-M_1 t}$$

$$-\frac{G_1}{\beta_1}e^{\beta_1 t}\left\{\sqrt{(M_1+\beta_1)}\left(erfc\left(\sqrt{(M_1+\beta_1)t}\right)-1\right)-\sqrt{a\beta_1}\left(erfc\left(\sqrt{a\beta_1 t}\right)-1\right)\right\}$$

$$+\lambda e^{\left(\frac{-1}{\lambda}\right)t}\left\{\sqrt{M_1-\frac{1}{\lambda}}\left(erfc\sqrt{\left(M_1-\frac{1}{\lambda}\right)t}-1\right)-\sqrt{\left(\frac{-a}{\lambda}\right)}\left(erfc\sqrt{a\left(\frac{-1}{\lambda}\right)t}-1\right)\right\}-G_2F_2 \quad (42)$$

$$Nu = \sqrt{\frac{a}{t\pi}} \quad (43)$$

$$Sh = -\sqrt{\frac{\mathrm{Sc}}{\pi t}} \quad (44)$$

2. Results and Discussion

We have explored an intriguing subject of unsteady MHD rotating waft of a fluid that is electrically performing, viscous, incompressible, and optically thick radiating Jeffrey's fluid. Our study focuses on the flow beyond an abruptly moving vertical plate that is embedded in a fluid inundated porous medium. We have also considered the temperature of the plate, which has a temporarily ramped profile. Behold, within the confines of this document lie felt a new depictions of scientific data. Observe with awe the figures numbered 2 through 10, as well as the illustrious 11 and 12. These visual aids unveil the secrets of velocity and temperature, both on ramped temperature and isothermal plates. And lo, the awareness profiles are also revealed in stunning detail.As the fluid flows over the plate, the primary velocity u and the secondary velocity w work in tandem to reach their peak performance close to of the plate's surface. From there, they gradually taper off, dutifully following the mounting boundary layer coordinate y as they make their way towards the space of free circulation evaluation.Furthermore, it can be perceived that the velocities of the primary and secondary fluids are comparatively lower in the ramped temperature plate configuration as compared to the isothermal plate configuration.

The frictional force, the Nusseltrange for bothramping temperatures and isothermal plates, and the Sherwood range have all been analysed and summarised within tables 1-3.Our observations indicate that Fig. 2 portrays the impact of a magnetic field on the primary pace (u) and secondary pace (w) under varying ramped temperatures and isothermal plate.The empirical evidence gleaned from Figs 2 and 3 indicates that, under both ramped temperature and isothermal conditions, the velocity components u and w exhibit a discernible decline as the Hartmann range M increases in proximity to the plate. This trend is observed to hold true across the spatial domain, both in the immediate vicinity of the plate and in the surrounding regions.The graphical representation in Fig 3 illustrates that the variables u and w exhibit a positive correlation with the permeability parameter k_0 across the fluid domain. A decrease in permeability slows the flow of fluid everywhere. Fig 4 depicted the impacts of rotation at the number one and secondary fluid velocities for plates

subjected to either ramping temperature or isothermal conditions.It is believed that the value of u will drop as R increases in proximity to the plate in the case of both ramping temperature plates and isothermal plates, whereas the value of w will increase as R increases in proximity to the plate. Rotation has an ability to keep the fluid moving at the returning number one velocity over the whole fluid location, and this holds true for both ramping temperature plates and isothermal plates.Despite the fact that in the field of flow, rotation is believed to have an effect on secondary fluid velocity by inhibiting the primary fluid velocity, this is not the case. Although it is generally accepted that rotation has a dampening effect on primary fluid velocity, which in turn affects secondary fluid velocity, in the flow discipline, only near the plate does it have a significant accelerating effect; farther away, its effect on the secondary fluid velocity is counteracting.This is owing to the fact that the pressure caused by Coriolis is more prominent within the region that is located close to the axis of rotation.It is obvious from the Figs.5 that both velocity components u and w increase with rising Jeffrey's fluid parameter for both ramping temperature and isothermal plates. This is something that stands out.Figs 6 and 7 show how thermal and mass diffusions affect the primary and secondary fluid velocity for ramped temperature and isothermal plates, respectively.In each of the situations, we found that u and w had a negative impact on the growth of Pr and Sc. So basically, thermal and mass diffusions cause the fluid velocities to speed up in the boundary layer region for both cases. This happens because thermal and mass diffusions push the thermal and awareness buoyancy forces forward.The figs eight and nine, which will illustrate the impact of thermal and concentration buoyancy forces upon the primary and secondary fluid velocities.It seems like u and w both increase as Gr and Gc increase, so basically, Gr is a measure of how much thermal buoyancy force there is compared to viscous pressure, and Gc is a measure of how much awareness buoyancy force there is compared to viscous pressure.As a consequence of this, the strengths of the thermal and attention buoyancy forces, respectively, continue to expand as Gr and Gc continue to flourish.Because of the influence of thermal and concentration buoyancy forces, natural convection float is encouraged in this case, and as a result, primary and secondary fluid velocities tend to increase near the boundary layer's immediate proximity.Figs. 10 showed the effects of thermal radiation on the primary and secondary fluid velocities for plates subjected to ramping temperature changes as well as isothermal conditions.In both cases, as N grows, so does u and w. In either scenario, it is possible that thermal radiation will speed up the number primary and secondary fluid velocities at some point in the boundary layer area.According to Figure Eleven, there is a positive correlation between the temperature and the size of N for both ramped temperature and isothermal plates.Therefore, in both circumstances, thermal radiation will be able to increase the fluid temperature in the boundary layer's immediate proximity. Hence thermal radiation offers diffuse energy, on account that an growth in N implies a decrease in Rosseland imply absorption coefficient k* for fixed values of and ok. Additionally it is reveal that fluid temperature decreases with increasing Pr. Therefore, in each cases, thermal diffusion tends to reinforce fluid temperature at some point of the boundary layer place. It's miles obvious from Figs.12 that species concentration diminishes with growing Sc whereas it complements on increasing t. Therefore mass diffusion has a tendency to increase attention and there's an improvement in concentration with boom of time in complete fluid vicinity.

The pores and skin friction increases and decreases with growing Hartmann quantity M for the ramped temperature, the reversal behaviour is found for isothermal plate. For the ramped temperature and isothermal plates reduces and will increase with increasing Gr, Gc, N and t, while increases and decreases with increasing Pr or Sc. Consequently, for ramped temperature and isothermal plates, thermal and awareness buoyancy forces, thermal and mass diffusions and thermal radiation have tendency to lessen whereas these bodily quantities have reverse effect on . For the ramped temperature and isothermal plates and increases with growing rotation parameter R or Jeffre’y fluid parameter. Rotation has a tendency to beautify both and for both ramped temperature and isothermal plates. Each and are growth for the ramped

temperature and decrease for isothermal plate on increasing permeability parameter okay (desk 1). The price of heat transfer reduces with increasing N and is augmented on increasing time for each cases, whereas it is dwindled to start with after which will increase with the boom of Pr (table 2). The Schmidt number to decorate price of mass switch on the plate and there is refuse in fee of mass transfer at the plate on increasing time (table three).

The outcomes are exact settlement with the consequences of Seth et al. [16] (desk 4).

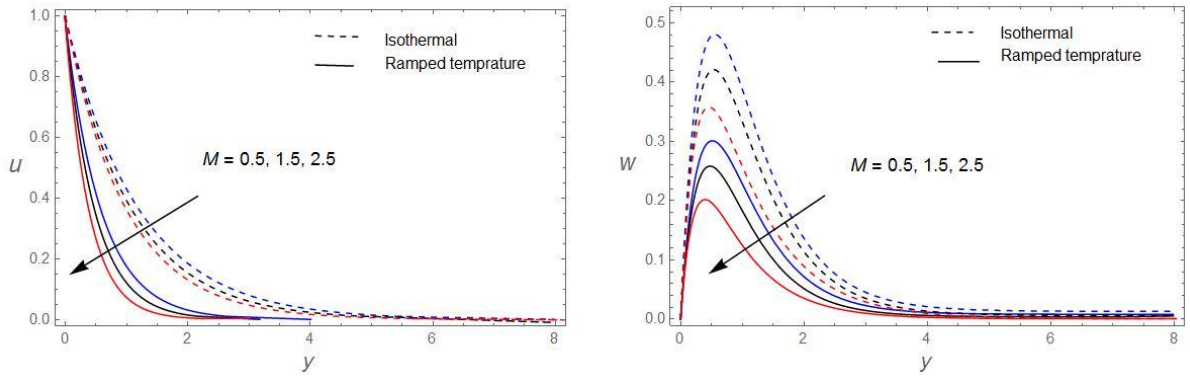

Fig. 2 The velocity profiles for *u*and*w*against*M* with
$R=1, K=0.5, \lambda=1, \Pr=0.71, N=2, \mathrm{Sc}=0.22, \mathrm{Gr}=3, \mathrm{Gc}=5, t=0.2$

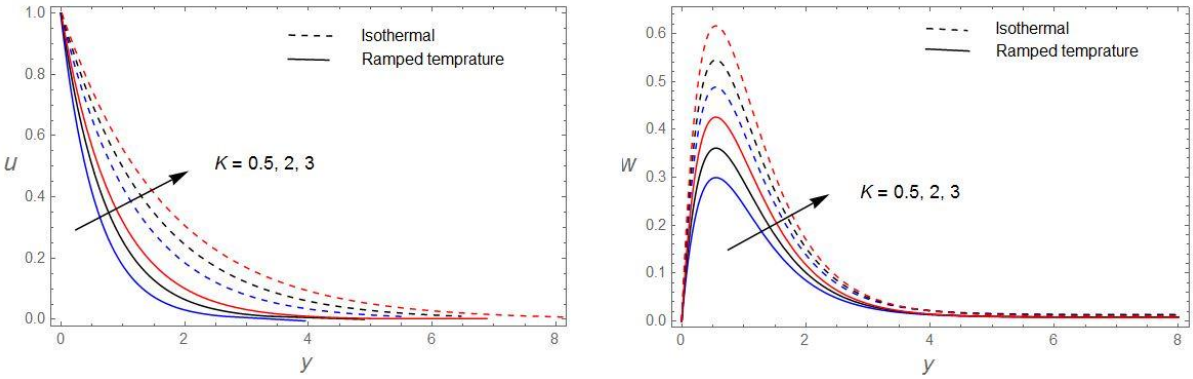

Fig. 3The velocity profiles for *u*and *w*against *K* with
$M=0.5, R=1, \lambda=1, \Pr=0.71, N=2, \mathrm{Sc}=0.22, \mathrm{Gr}=3, \mathrm{Gc}=5, t=0.2$

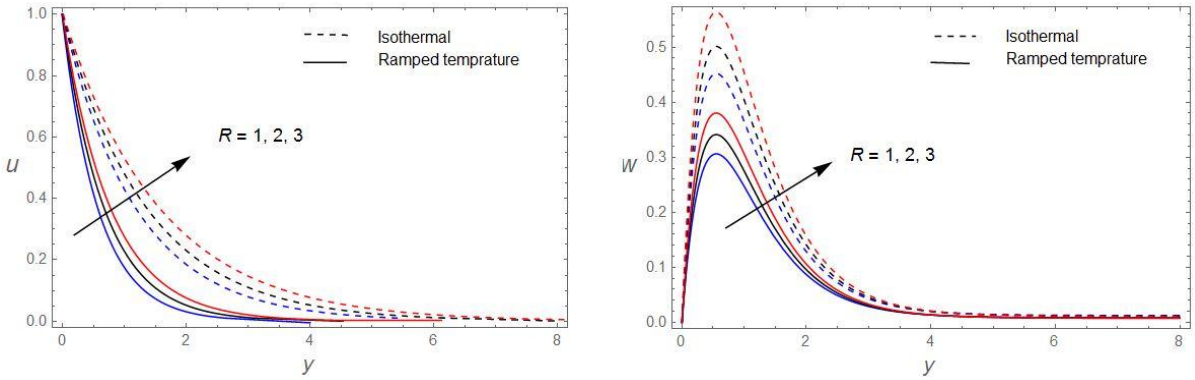

Fig. 4The velocity profiles for *u*and *w* against *R* with
$M=0.5, K=0.5, \lambda=1, \Pr=0.71, N=2, \mathrm{Sc}=0.22, \mathrm{Gr}=3, \mathrm{Gc}=5, t=0.2$

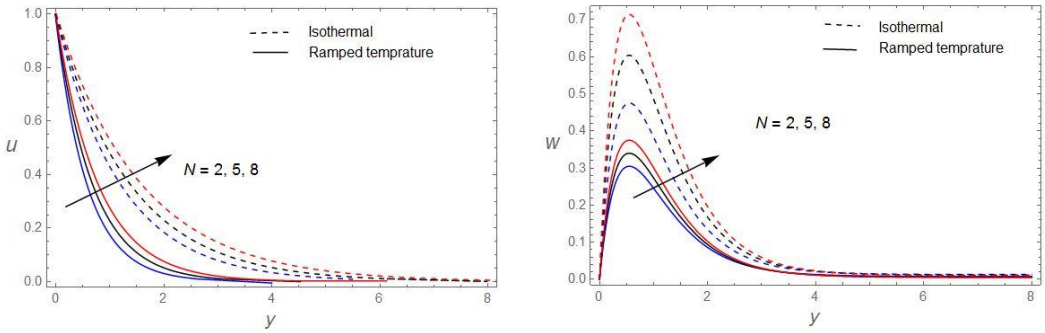

Fig. 5The velocity profiles for *u* and *w* against λ with
$M = 0.5, R = 1, K = 0.5, \Pr = 0.71, N = 2, \mathrm{Sc} = 0.22, \mathrm{Gr} = 3, \mathrm{Gc} = 5, t = 0.2$

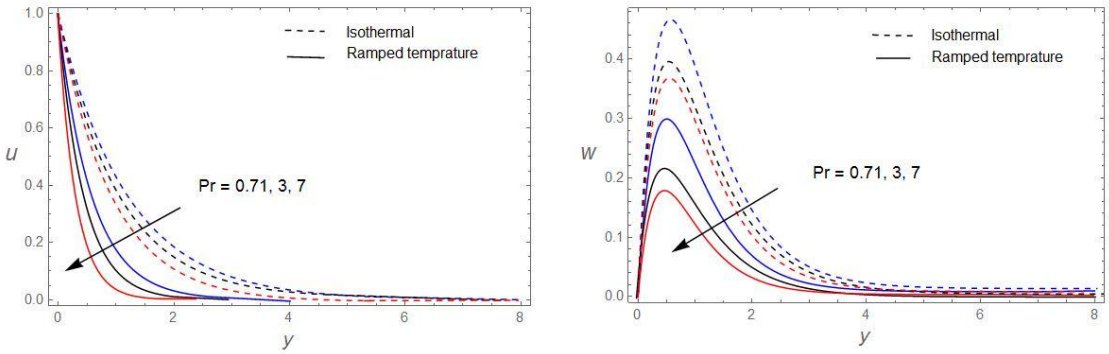

Fig. 6The velocity profiles for *u*and *w*against Pr with
$M = 0.5, R = 1, K = 0.5, \lambda = 1, N = 2, \mathrm{Sc} = 0.22, \mathrm{Gr} = 3, \mathrm{Gc} = 5, t = 0.2$

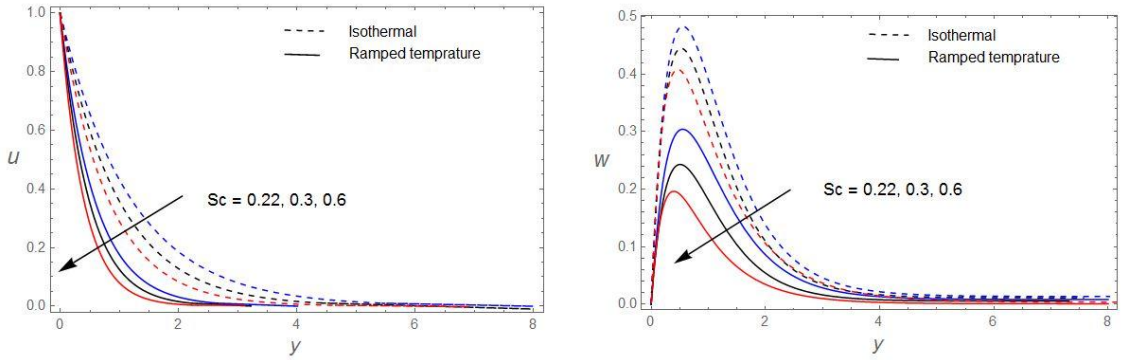

Fig. 7The velocity profiles for *u*and *w*against Sc with
$M = 0.5, R = 1, K = 0.5, \lambda = 1, \Pr = 0.71, N = 2, \mathrm{Gr} = 3, \mathrm{Gc} = 5, t = 0.2$

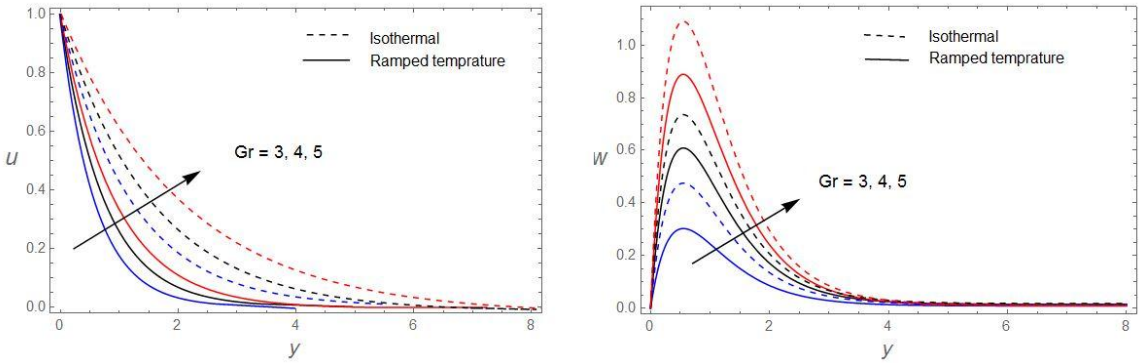

Fig. 8The velocity profiles for *u* and *w* against Gr with
$M = 0.5, R = 1, K = 0.5, \lambda = 1, \Pr = 0.71, N = 2, \mathrm{Sc} = 0.22, \mathrm{Gc} = 5, t = 0.2$

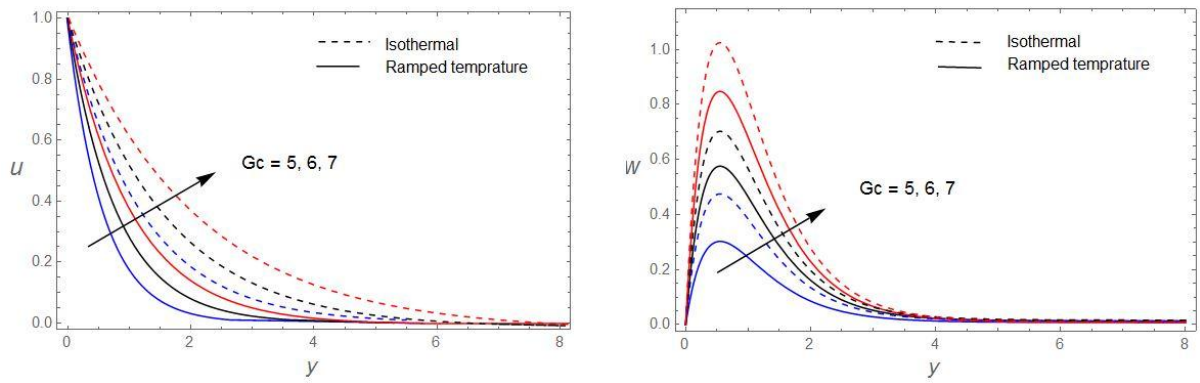

Fig. 9The velocity profiles for *u*and *w*against Gc with
$M = 0.5, R = 1, K = 0.5, \lambda = 1, \Pr = 0.71, N = 1, \mathrm{Sc} = 0.22, \mathrm{Gr} = 3, t = 0.2$

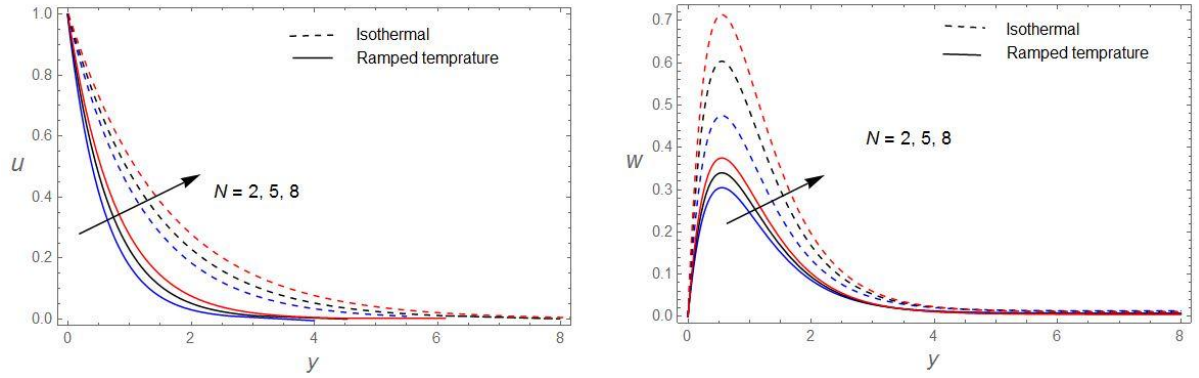

Fig. 10The velocity profiles for *u*and *w*against *N* with
$M = 0.5, R = 1, K = 0.5, \lambda = 1, \Pr = 0.71, \mathrm{Sc} = 0.22, \mathrm{Gr} = 3, \mathrm{Gc} = 5, t = 0.2$

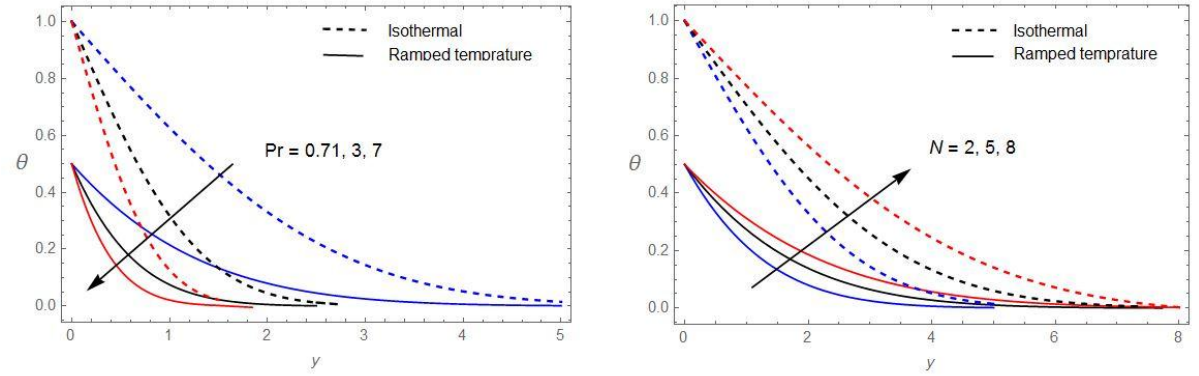

Fig. 11The temperature profiles against Pr and *N* with *t* = 0.5

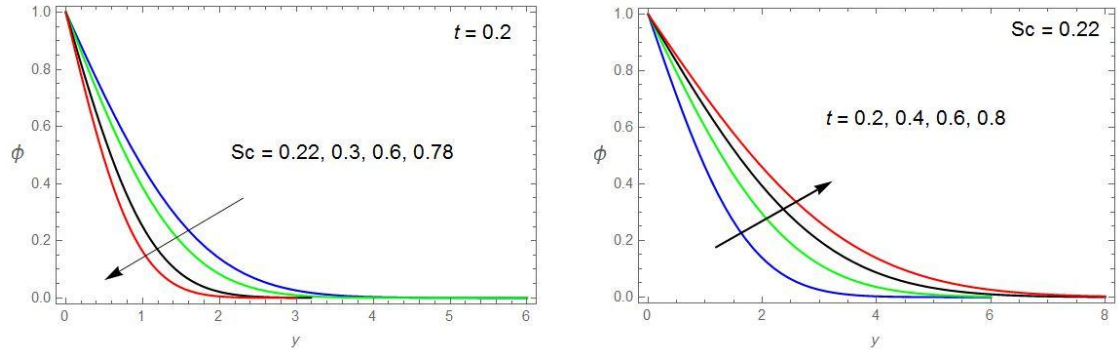

Fig. 12The concentration profiles against Sc and *t*

Table 1: Skin friction

M	K	R		λ	Pr	Gr	Gc	N	Sc	t	Ramped $-\tau_x$	temperature τ_z	Isothermal $-\tau_x$	plate τ_z
0.5	0.5	1		1	0.71	3	5	2	0.22	0.2	2.86522	1.99985	2.16589	2.42544
1											3.15225	1.55244	1.87785	2.67025
1.5											3.42011	1.36522	1.71445	2.88547
	1										3.26558	2.33566	1.71662	1.86485
	1.5										3.65774	2.67588	1.25524	1.42415
		2									3.26658	2.15447	2.49969	2.86550
		3									3.66322	2.59855	2.88858	3.23324
				2							3.12100	2.30142	2.49996	2.89965
				3							3.53214	2.63552	2.96638	3.15526
					3						3.33255	1.83526	2.34255	2.23255
					7						3.67455	1.71145	2.62855	2.02256
						4					2.57885	2.34625	2.06658	2.67588
						5					2.02544	2.51774	1.89965	2.82145
							6				2.46988	2.16522	1.89899	2.86635
							7				2.15547	2.37996	1.53365	3.22214
								3			2.72011	2.00115	2.02144	2.46585
								4			2.61477	2.01552	1.90225	2.48854
									0.3		3.00144	1.81145	2.36556	2.23232
									0.6		3.15244	1.66636	2.53985	2.02565
										0.5	2.72104	2.14225	2.02114	2.96558
										0.8	2.52145	2.42885	1.96699	3.21044

Table 2: Nusselt number

N	Pr	t	Nu Ramped temperature	Nu Isothermal plate
2	0.71	0.5	0.274469	0.194079
5			0.194079	0.137235
8			0.158465	0.112052
	3		0.164682	0.150333
	7		0.439151	0.245493
		0.3	0.564190	0.398942
		0.8	0.861814	0.609394

Table 3: Sherwood number

Sc	***t***	**Sh**
0.22	0.2	-0.591727
0.3		-0.690988
0.6		-0.977205
0.78		-1.114190
	0.4	-0.418414
	0.6	-0.341634
	0.8	-0.295864

Table 4: Results comparison for the Primary velocity component (u) ($\mathrm{Gc}=5, \mathrm{Pr}=0.71, \mathrm{Sc}=0.22,\ z=0.5, t=0.2$)

M	K	R	N	Previous results Seth et al.[16]	Present Results $\lambda=0$
0.5	0.5	1	2	0.223458	0.223469
1				0.214452	0.214463
1.5				0.203145	0.203156
	1.0			0.241152	0.241164
	1.5			0.259478	0.259489
		2		0.250214	0.250225
		3		0.289960	0.289974
			3	0.240155	0.240169
			4	0.261044	0.261058

3. Conclusions

We have discussed unsteady MHD rotating go with the flow of an electrically engaging in, viscous, incompressible and optically thick radiating Jeffrey's fluid beyond an impulsively vertical transferring porous plate. The conclusions are made for each ramped temperature and isothermal plates, consequences of rotation has a tendency to accelerate w and slow down u for the duration of the boundary layer area. Thermal and attention buoyancy forces, thermal and mass diffusions and thermal radiation tend to accelerate both speed components. Thermal radiation and thermal diffusion has a tendency to enhance fluid temperature in the course of the boundary layer area. Mass diffusion has a tendency to beautify concentration at some point of the boundary layer area. Thermal and concentration buoyancy forces, thermal diffusions and thermal radiation have tendency to reduce primary pressure issue while these physical portions have reverse effect on secondary stress issue. Rotation and Jeffrey's fluid parameters generally tend to enhance each pressure additives. Price of heat transfer reduces with increasing N and is augmented on increasing time. The Schmidt number is to decorate mass transfer on the plate and refuses on increasing time.

4. References

[1]. Bejan A (1993), Convection heat transfer, 2nd ed,NY: Wiley.

[2]. Gebhart B, Pera L (1971), The nature of vertical natural convection flowsresulting from the combined buoyancy effects of thermal and massdiffusion,*Int J Heat Mass Transfer*, 14, 2025–50.

[3]. RaptisA.A(1982), Free convection and mass transfer effects on theoscillatory flow past an infinite moving vertical isothermal platewith constant suction and heat sources,*Astrophy Space Sci*, 86, 43–53.

[4]. Bejan A, Khair K.R (1985), Heat and mass transfer by natural convectionin a porous medium. *Int J Heat Mass Transfer*, 28, 909–18.

[5]. Jang JY, Chang W.J (1988), Buoyancy-induced inclined boundary layerflow in a porous medium resulting from combined heat and massbuoyancy effects. *IntCommun Heat Mass Transfer*, 15, 17–30.

[6]. Lai F.C, Kulacki F.A. (1991),Non-Darcy mixed convection along avertical wall in a saturated porous medium. *J Heat Transfer*, 113, 252–5.

[7]. Nakayama A, Hossain M.A.(1995), An integral treatment for combinedheat and mass transfer by natural convection in a porous medium,*Int J Heat Mass Transfer*, 38, 761–5.

[8]. Yih K.A.(1997), The effect of transpiration on coupled heat and masstransfer in mixed convection over a vertical plate embedded in asaturated porous medium,*IntCommun*

[9]. Jayalakshmi P, Gangadhar K, Obulesu M, Madhu Mohan Reddy P. The axisymmetric flow of an MHD Powell–Eyring fluid with viscous dissipation and Newtonian heating condition: keller-box method. Heat Transfer. 2022;1-13. doi:10.1002/htj.22723

[10]. Chamkha A.J, Takhar H.S, Soundalgekar V.M. (2001), Radiation effectson free convection flow past a semi-

infinite vertical plate withmasstransfer,*ChemEng J*, 84, 335–42.

[11]. Ganesan P, Palani G. (2003), Natural convection effects on impulsivelystarted inclined plate with heat and mass transfer,*HeatMassTransfer*, 39, 277–83.

[12]. Eckert E.R, Drake R.M. (1972), Analysis of heat and mass transfer. NY:Mc-Graw Hill.

[13]. Gebhart B, Jaluria Y, Mahajan R.L, SammakiaB.(1998),*BuoyancyInduced Flow and Transport*, New York, Hemisphere.

[14]. Yu-Ming Chu, FarisAlzahrani, ObulesuMopuri, CharankumarGanteda, M.Ijaz Khan, P. Jaya lakshmi, Sami Ullah Khan, Sayed M. Eldin, Thermal impact of hybrid nanofluid due to inclined oscillatory porous surface with thermo-diffusion features, Case Studies in Thermal Engineering, Volume 42,2023, 102695, ISSN 2214-157X, https://doi.org/10.1016/j.csite.2023.102695.

[15]. Pop I, Ingham.D.B.(2001),*Convective heat transfer: mathematical andcomputational modelling of viscous fluids and porous media*.,Oxford: Pergamon.

[16]. Seth, G.S., Sarkar, S., Hussian, S.M., Effects of Hall current, Radiation and rotation on natural convection heat and mass transfer flow past a moving vertical plate, Ain Shams Engineering Journal, 5, 489-503, 2014. http://dx.doi.org/10.1016/j.asej.2013.09.014

[17]. Mohamed Abd El-Aziz, Dual solutions in hydromagnetic stagnation point flow and heat transfer towards a stretching/shrinking sheet with non-uniform heat source/sink and variable surface heat flux, Journal of the Egyptian Mathematical Society, 24(3), 479-486, 2016.https://doi.org/10.1016/j.joems.2015.09.004

[18]. AzeemShahzad, Ramzan Ali, MurrawatHussain, Muhammad Kamran, Unsteady axisymmetric flow and heat transfer over time-dependent radially stretching sheet, Alexandria Eng. J. 56(1), 35-41, 2016. https://doi.org/10.1016/j.aej.2016.08.030

[19]. Turkyilmazoglu, Flow of a micropolar fluid due to a porous stretching sheet and heat transfer, International Journal of Non-Linear Mechanics, 83, 59-64, 2016. https://doi.org/10.1016/j.ijnonlinmec.2016.04.004

[20]. S. Baag, S.R. Mishra, G.C. Dash, M.R. Acharya, Entropy generation analysis for viscoelastic MHD flow over a stretching sheet embedded in a porous medium, Ain Shams Engineering Journal, 8(4), 623-632, 2016. https://doi.org/10.1016/j.asej.2015.10.017

[21]. Jawad Ahmed, Abida Begum, AzeemShahzad, Ramzan Ali, MHD axisymmetric flow of power-law fluid over an unsteady stretching sheet with convective boundary conditions, Results in Physics, 6, 973-981, 2016. https://doi.org/10.1016/j.rinp.2016.11.013

[22]. N.F. Fauzi, S. Ahmad, I. Pop, Stagnation point flow and heat transfer over a nonlinear shrinking sheet with slip effects, Alexandria Engineering Journal, 54(4), 929-934,2015.https://doi.org/10.1016/j.aej.2015.08.004

[23]. A.K. Abdul Hakeem, N. Vishnu Ganesh, B. Ganga, Magnetic field effect on second order slip flow of Nano fluid over a stretching/shrinking sheet with thermal radiation effect, Journal of Magnetism and Magnetic Materials, 381,243-257, 2015. https://doi.org/10.1016/j.jmmm.2014.12.010

[24]. RuchikaDhanai, PuneetRana, Lokendra Kumar, Multiple solutions of MHD boundary layer flow and heat transfer behavior of nanofluids induced by a power-law stretching/shrinking permeable sheet with viscous dissipation, Powder Technology, 273, 62-70, 2015.https://doi.org/10.1016/j.powtec.2014.12.035

[25]. K. Bhattacharyya, I. Pop, MHD Boundary layer flow due to an exponentially shrinking sheet, Magnetohydrodynamics, 47(4),337-344, 2011.

[26]. K. Bhattacharyya, Effects of heat source/sink on MHD flow and heat transfer over a shrinking sheet with mass suction, Chem. Eng. Res. Bull. 15(1), 12-17, 2011. https://doi.org/10.3329/cerb.v15i1.6524

[27]. K. Bhattacharyya, Effects of radiation and heat source/sink on unsteady MHD boundary layer flow and heat transfer over a shrinking sheet with suction/injection, Front. Chem. Sci. Eng. 5, 376-384, 2011.https://doi.org/10.1007/s11705-011-1121-0

[28]. Gangadhar, Kotha, T. Kannan, and P. Jayalakshmi."Magnetohydrodynamicmicropolarnanofluid past a permeable stretching/shrinking sheet with Newtonian heating." Journal of the Brazilian Society of

Mechanical Sciences and Engineering 39, no. 11 (2017): 4379-4391.

[29]. Maria Imtiaz, Tasawar Hayat, Ahmed Alsaedi, MHD convective flow of Jeffrey fluid due to a curved stretching surface with homogeneous-heterogeneous reactions. PLoS ONE 11(9), e0161641, 2016. https://doi.org/10.1371/journal.pone.0161641

[30]. N. Sandeep, C. Sulochana, Momentum and heat transfer behaviour of Jeffrey, Maxwell and Oldroyd-B nanofluids past a stretching surface with non-uniform heat source/sink, Ain Shams Eng. Journal. 9(4), 517-524, 2016. https://doi.org/10.1016/j.asej.2016.02.008

[31]. Kartini Ahmad, ZahirHanouf, and AnuarIshak, Mixed convection Jeffrey fluid flow over an exponentially stretching sheet with magnetohydrodynamic effect, AIP Advances 6(3), 035024, 2016. https://doi.org/10.1063/1.4945401

[32]. Tasawar Hayat, Muhammad Waqas, Sabir Ali Shehzad, Ahmed Alsaedi, MHD stagnation point flow of Jeffrey fluid by a radially stretching surface with viscous dissipation and Joule Heating, J. Hydrol. Hydromech., 63(4), 311-317, 2015. https://doi.org/10.1515/johh-2015-0038

[33]. Kalidas Das a, Nilangshu Acharya, Prabir Kumar Kundu, Radiative flow of MHD Jeffrey fluid past a stretching sheet with surface slip and melting heat transfer, Alexandria Engineering Journal, 54(4), 815-821, 2015. https://doi.org/10.1016/j.aej.2015.06.008

[34]. Free convective oscillatory flow due to inclined perpendicular shield subject to the thermos-diffusion and suction effects, Heliyon, 9(4), 2023 https://doi.org/10.1016/j.heliyon.2023.e14781

[35]. Applications of variable plastic viscosity and thermal conductivity for Casson fluid source. with slip effects and space dependent internal heat generation, Journal of the Indian chemical society, 99(10),2022, https://doi.org/10.1016/j.jics.2022.100712

[36]. MHD casson fluid flow past a stretching sheet with convective boundary and heat Lecture notes in Mechanical Engineering 2021,pp: 559-572, https://doi.org/10.1007/978-981-15-4308-1_44

[37]. MHD convective flow through porous medium in a horizontal channel with insulated and impermeable bottom wall in the presence of viscous dissipation and joule heating, Ain shams engineering journal,5(2),pp: 543-551, 2014, https://doi.org/10.1016/j.asej.2013.10.007

Appendix:

$$M_1 = \frac{M^2}{1-im} + \frac{1}{K} - 2iR^2,\ a = \frac{\Pr}{1+N},\ G_3 = \frac{Gc}{M_1},\ \gamma = G_1\left(\frac{1}{\beta_1} - \lambda\right),$$

$$\theta^*(y,t) = \left(t + \frac{ay^2}{2}\right) erfc\left(\frac{y}{2}\sqrt{\frac{a}{2}}\right) - \sqrt{\frac{at}{\pi}}\ y\ e^{-\frac{ay^2}{4t}}$$

$$F^*(y,t) = \frac{1}{2}\left\{\frac{e^{\beta_1 t}}{\beta_1^2}\left(e^{y\sqrt{(\lambda+\beta_1)}} erfc\left(\frac{y}{2\sqrt{t}} + \sqrt{(\lambda+\beta_1)t}\right) + e^{-y\sqrt{(\lambda+\beta_1)}} erfc\left(\frac{y}{2\sqrt{t}} - \sqrt{(\lambda+\beta_1)t}\right)\right.\right.$$

$$\left.\left. - e^{y\sqrt{(a\beta_1)}} erfc\left(\frac{y}{2}\sqrt{\frac{a}{t}} + \sqrt{\beta_1 t}\right) - e^{-y\sqrt{(a\beta_1)}} erfc\left(\frac{y}{2}\sqrt{\frac{a}{t}} - \sqrt{\beta_1 t}\right)\right)\right.$$

$$\left. - \frac{1}{\beta_1}\left\{\left(t + \frac{1}{\beta_1} + \frac{y}{2\sqrt{\lambda}}\right) e^{y\sqrt{\lambda}} erfc\left(\frac{y}{2\sqrt{t}} + \sqrt{\lambda t}\right) + \left(t + \frac{1}{\beta_1} - \frac{y}{2\sqrt{\lambda}}\right) e^{-y\sqrt{\lambda}} erfc\left(\frac{y}{2\sqrt{t}} - \sqrt{\lambda t}\right)\right.\right.$$

$$\left.\left. - 2\left(t + \frac{1}{\beta_1} + \frac{ay^2}{2}\right) erfc\left(\frac{y}{2}\sqrt{\frac{a}{t}}\right) + 2\sqrt{\frac{at}{\pi}}\ ye^{-\frac{ay^2}{4t}}\right\}\right.$$

$$+\lambda^2\ e^{\left(\frac{-1}{\lambda}\right)t}\left(e^{y\sqrt{y-\frac{1}{\lambda}}}\ erfc\left(\frac{y}{2\sqrt{t}}+\sqrt{\left(M_1-\frac{1}{\lambda}\right)t}\right)+e^{-y\sqrt{y-\frac{1}{\lambda}}}\ erfc\left(\frac{y}{2\sqrt{t}}-\sqrt{\left(M_1-\frac{1}{\lambda}\right)t}\right)\right.$$

$$\left.-e^{y\sqrt{\frac{-a}{\lambda}}}\ erfc\left(\frac{y}{2}\sqrt{\frac{a}{t}}+\sqrt{\left(\frac{-1}{\lambda}\right)t}\right)-e^{-y\sqrt{\frac{-a}{\lambda}}}\ erfc\left(\frac{y}{2}\sqrt{\frac{a}{t}}-\sqrt{\left(\frac{-1}{\lambda}\right)t}\right)\right)\ \Bigg\}$$

$$\phi^*(y,t)=\frac{1}{2\beta_2(1-\beta_2\lambda)}$$

$$\left(e^{y\sqrt{M_1}}erfc\left(\frac{y}{2\sqrt{t}}+\sqrt{M_1 t}\right)+e^{-y\sqrt{M_1}}\ \ erfc\left(\frac{y}{2\sqrt{t}}-\sqrt{M_1 t}\right)-2erfc\left(\frac{y}{2}\sqrt{\frac{\mathrm{Sc}}{t}}\right)\right.$$

$$-e^{-\beta_2 t}\left\{e^{y\sqrt{\frac{M_1-\beta_2}{1-\beta_2\lambda}}}erfc\left(\frac{y}{2\sqrt{t}}+\sqrt{\left(\frac{M_1-\beta_2}{1-\beta_2\lambda}\right)t}\right)+e^{-y\sqrt{\frac{M_1-\beta_2}{1-\beta_2\lambda}}}erfc\left(\frac{y}{2\sqrt{t}}-\sqrt{\left(\frac{M_1-\beta_2}{1-\beta_2\lambda}\right)t}\right)\right.$$

$$-e^{iy\sqrt{\mathrm{Sc}\ \beta_2}}\ erfc\left(\frac{y}{2}\sqrt{\frac{\mathrm{Sc}}{t}}+i\sqrt{\beta_2 t}\right)-e^{-iy\sqrt{\mathrm{Sc}\ \beta_2}}\ erfc\left(\frac{y}{2}\sqrt{\frac{\mathrm{Sc}}{t}}-i\sqrt{\beta_2 t}\right)$$

$$\left.\left.-e^{iy\sqrt{\mathrm{Sc}\ (-1/\lambda)}}\ erfc\left(\frac{y}{2}\sqrt{\frac{\mathrm{Sc}}{t}}+i\sqrt{(-1/\lambda)t}\right)-e^{-iy\sqrt{\mathrm{Sc}\ (-1/\lambda)}}\ erfc\left(\frac{y}{2}\sqrt{\frac{\mathrm{Sc}}{t}}-i\sqrt{(-1/\lambda)t}\right)\right\}\right)$$

$$\phi_1^*=\frac{1}{2}\left\{\left(t+\frac{y}{2\sqrt{M_1}}\right)e^{y\sqrt{M_1}}erfc\left(\frac{y}{2\sqrt{t}}+\sqrt{M_1 t}\right)+\right.$$

$$\left.+\left(t-\frac{y}{2\sqrt{M_1}}\right)e^{-y\sqrt{\lambda}}erfc\left(\frac{y}{2\sqrt{t}}-\sqrt{M_1 t}\right)-2erfc\left(\frac{y}{2\sqrt{t}}\right)\right\}$$

$$F_1(0,t)=\frac{e^{\beta_1 t}}{\beta_1^2}\left[\sqrt{(M_1+\beta_1)}\left\{erfc(\sqrt{(M_1+\beta_1)t})-1\right\}-\sqrt{a\beta_1}\left\{erfc(\sqrt{\beta_1 t})-1\right\}\right]$$

$$-\lambda^2 e^{-\left(\frac{1}{\lambda}\right)t}\left[\sqrt{\left(M_1-\frac{1}{\lambda}\right)}\left\{erfc\left(\sqrt{\left(M_1-\frac{1}{\lambda}\right)t}\right)-1\right\}-\sqrt{a\left(\frac{-1}{\lambda}\right)}\left\{erfc\left(\sqrt{\left(\frac{-1}{\lambda}\right)t}\right)-1\right\}\right]$$

$$+\frac{\lambda}{\beta_1}\left[\left\{\left(t+\frac{1}{\beta_1}-\lambda\right)\sqrt{M_1}+\frac{1}{2\sqrt{M_1}}\right\}\left\{erfc(\sqrt{M_1 t})-1\right\}-\sqrt{\frac{t}{\pi}}\left(e^{-M_1 t}-\sqrt{a}\right)\right]$$

$$F_2(0,t)=\frac{-\lambda}{\beta_2}\left(\sqrt{M_1}\left\{erfc(\sqrt{M_1 t})-1\right\}+\frac{1}{\sqrt{\pi t}}\left(2\sqrt{\mathrm{Sc}}-1\right)-\right.$$

$$-e^{-\beta_2 t}\left\{\sqrt{M_1-\beta_2}\left(erc\sqrt{(M_1-\beta_2)t}-1\right)-i\sqrt{\mathrm{Sc}\,\beta_2}\left(erfc\sqrt{i\beta_2 t}-1\right)\right\}$$

$$\left.-e^{-\left(\frac{1}{\lambda}\right)t}\left\{\sqrt{M_1+\frac{1}{\lambda}}\left(erf\sqrt{\left(M_1+\frac{1}{\lambda}\right)t}-1\right)-i\sqrt{\frac{\mathrm{Sc}}{\lambda}}\left(erfc\sqrt{i\left(\frac{-1}{\lambda}\right)t}-1\right)\right\}\right)$$